

**AAS 12-106**



**MULTI SPHERE MODELING FOR  
ELECTROSTATIC FORCES ON  
THREE-DIMENSIONAL SPACECRAFT SHAPES**

**Daan Stevenson and Hanspeter Schaub**

**AAS/AIAA Space Flight Mechanics  
Meeting**

**Charleston, South Carolina**

**January 29 – February 2, 2012**

**AAS Publications Office, P.O. Box 28130, San Diego, CA 92198**

# MULTI SPHERE MODELING FOR ELECTROSTATIC FORCES ON THREE-DIMENSIONAL SPACECRAFT SHAPES

Daan Stevenson\* and Hanspeter Schaub†

The use of electrostatic (Coulomb) actuation for formation flying is attractive because non-renewable fuel reserves are not depleted and plume impingement issues are avoided. Prior analytical electrostatic force models used for Coulomb formations assume spherical spacecraft shapes, which include mutual capacitance and induced effects. However, this framework does not capture any orientation dependent forces or torques on generic spacecraft geometries encountered during very close operations and docking scenarios. The Multi Sphere Model (MSM) uses a collection of finite spheres to represent a complex shape and analytically approximate the Coulomb interaction with other charged bodies. Finite element analysis software is used as a truth model to determine the optimal MSM parameters. The model is robust to varying system parameters such as prescribed voltages and external shape size. Using the MSM, faster-than-realtime electrostatic simulation of six degree of freedom relative spacecraft motion is feasible, which is crucial for the development of robust relative position and orientation control algorithms in local space situational awareness applications.

## INTRODUCTION

As the complexity of spaceflight missions increases, formation flying scenarios can provide beneficial contributions to the science objectives and insurance of mission success. Conventionally, relative position maneuvers are performed using external thrusters that convert fuel into exhaust plumes directed into space. One obvious drawback of this type of propulsion is the costly expenditure of non-renewable fuel reserves, especially in high accuracy relative orbits where frequent position corrections are necessary. Moreover, there is potential for exhaust plume impingement, where thruster exhaust from one craft causes interference with its neighbor's sensors. An attractive alternative is the recently emerging Coulomb charge control technology. The electrostatic potential of multiple spacecraft can be controlled within microseconds using electro-gun or cathode devices, and the resulting Coulomb forces can be used to affect relative spacecraft positions within a formation.<sup>1,2,3,4</sup>

Applications of Coulomb charge control include Separated Spacecraft Interferometry (SSI), to achieve large field-of-view planetary imagery with unprecedented resolution, spacecraft docking by electrostatic tractor concepts, and small-body relative orbits with cameras or other robotic devices to inspect external spacecraft integrity. Electrostatic tugs may also be used to deorbit space debris, for if a spacecraft can impart relative potentials on itself and a foreign craft using a focused charged beam, touchless re-orbiting maneuvers may be achieved.<sup>5,6,7</sup> One limitation of this technology is

\*Graduate Student, Aerospace Engineering Sciences, University of Colorado.

†Associate Professor, H. Joseph Smead Fellow, Department of Aerospace Engineering Sciences, University of Colorado, 431 UCB, Colorado Center for Astrodynamics Research, Boulder, CO 80309-0431.

the effect of plasma in the near-Earth space environment, which causes considerable Debye shielding of the electrostatic fields at LEO. Spacecraft formations at GEO, however, can exert significant electrostatic forces at separation distances of tens of meters, because the Debye lengths there range from 180-200 meters.<sup>1,8,9</sup>

Several studies analyze the relative motion dynamics of a 2 to  $N$  craft Coulomb formation.<sup>10,11,12</sup> Complex charge control strategies have been developed that compensate for the nonlinear nature of the electrostatic forces and coupling with differential gravity.<sup>13,14,15,16</sup> In such work spacecraft electrostatics are generally modeled by point charges, while in actuality a voltage is prescribed by the charge control methods. The electrostatic charge density on the conducting surface is then a result of the spacecraft geometry and external potential fields. For experimental verification of relative motion by Coulomb charge control, physical conducting spheres are used to represent spacecraft bodies.<sup>17,18</sup> To model these interactions, both the mutual capacitance between conducting spheres<sup>19,20</sup> and induced charging effects<sup>21</sup> are considered to determine the voltage to charge relationship.

Realistically, spacecraft components such as solar panels result in geometries that are far from spherical. When charged bodies interact with separation distances on the order of the spacecraft dimensions, especially in the small body circumnavigation scenario, a model that assumes spherical conductors can result in considerable errors in the electrostatic force prediction. Charge prediction errors of 10% (which can easily result from geometry approximations) have been shown to cause up to 15% errors in relative position control.<sup>7</sup> Reference 22 proposes to overcome these inaccuracies with an Effective Sphere Method (ESM). Here a finite sphere is used to model the spacecraft body using an effective radius that best captures the electrostatic response over a range of separation distances to an external object. If expanded to 1st order, the effective radius can change depending on spacecraft orientation to capture non-spherical effects. While this approach allows for a very simple analytical force prediction, it compromises accuracy of the Coulomb force at small spacecraft separation distances. Perhaps more importantly, the ESM lacks the ability to resolve electrostatic torques and non line-of-sight forces that result from non-symmetric spacecraft bodies. This is crucial when relative attitudes and small separation distances on the order of the spacecraft dimensions are a consideration in the formation flight mission scenario.

This paper introduces a new approach called the Multi Sphere Model (MSM). Essentially, the electrostatics of a spacecraft with a conducting outer surface held at a fixed voltage is approximated by filling the geometry with multiple finite spheres held at a constant voltage. Because the charge on each sphere is allowed to vary as determined by the mutual capacitance matrix, a similar freedom in the charge distribution throughout the spacecraft is seen as in a generic conducting geometry. As such, the model is robust for various orientations and separation distances, while the accuracy of the model depends on how many spheres are used. The challenge with the MSM is in choosing the size and location of a prescribed number of spheres for a given spacecraft shape. The truth model used for this purpose is Ansoft's Finite Element Method (FEM) software suite Maxwell 3D ©. FEM creates a highly accurate but computationally expensive solution of the electrostatic potential fields by creating linearized solutions for Poisson's equation on each finite element in the entire 3D space, with boundary conditions created from the spacecraft geometries and potentials. On their own, the FEM solvers are not capable of faster-than-realtime charged relative motion simulations, and therefore do not provide analytical insight into the dynamics and control of such scenarios.

The MSM methodology, by comparison, resolves forces and torques on the body by iterating Coulomb's law over the charge found on each sphere in the model due to their mutual and self capacitance. This paper examines how to determine best-fit MSM parameters for a general shape, and

discusses the accuracies and limitations of this approach. Further, numerical simulations illustrate how this model can be applied to study the use of electrostatic torque to change the spin of a passive body.

## MULTI SPHERE MODEL THEORY

The Multi Sphere Model (MSM) is a method to approximate the electrostatic interactions between conducting objects with generic geometries. A rigid spacecraft or space debris object is modeled by a collection of spheres with fixed sizes and relative positions, as shown in Figure 1. Generally, an external sphere is used to resolve the forces and torques on the body so that an optimal solution of the model parameters can be determined. In this section, we assume that the optimal relative positions and sizes of the  $n$  spheres in the model has already been determined, for which the process is discussed in the following section. Once these parameters are known, the electrostatic dynamics of a modeled spacecraft can be predicted by replacing its geometry with the finite spheres, which are constrained to match the translation and rotation of the actual body. At this point the external sphere can also be replaced by another generic geometry represented by a MSM.

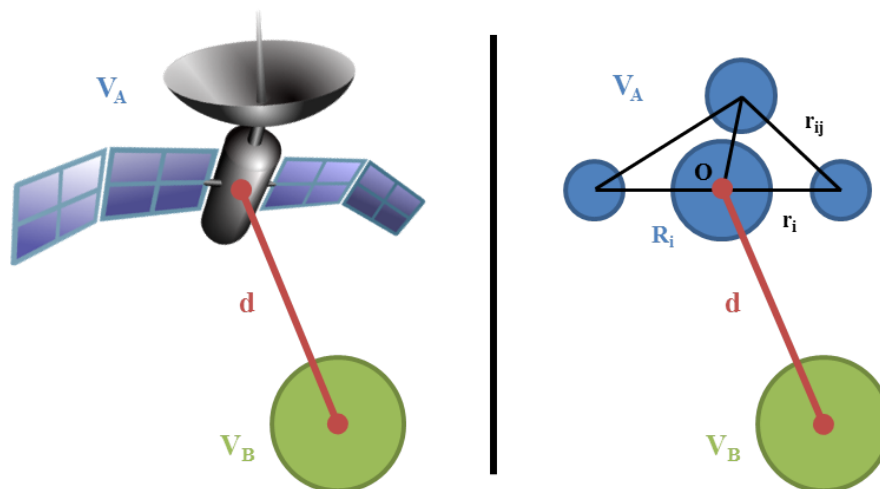


**Figure 1. Conceptual depiction of Multi Sphere Method**

While the absolute electrostatic voltage is assumed to be prescribed on a spacecraft, the Coulomb force between the spheres is dependent on the charge that each holds. The voltage  $V_i$  on a given sphere is a result of both the charge on that sphere and the charges on its neighboring spheres. The relation is given in Eq. (1),<sup>19,20</sup> where  $R_i$  represents the radius of the sphere in question and  $\mathbf{r}_{i,j} = \mathbf{r}_j - \mathbf{r}_i$  is the center-to-center distance to each neighbor. The constant  $k_c = 8.99 \times 10^9 \text{ Nm}^2/\text{C}^2$  is Coulomb's constant, and  $q_i$  stands for the charge on a given sphere.

$$V_i = k_c \frac{q_i}{R_i} + \sum_{j=1, j \neq i}^m k_c \frac{q_j}{r_{i,j}} \quad (1)$$

The linear relations for each of the  $m = n + 1$  spheres in the system ( $n$  spheres in the MSM plus the external sphere) can be combined in the matrix form of Eq. (2), where  $\mathbf{V} = [V_A, V_A, \dots, V_A, V_B]^T$

and  $\mathbf{q} = [q_1, q_2, \dots, q_n, q_B]^T$  represent matrix collections of the voltages and charges in the entire system.

$$\mathbf{V} = k_c [C_M]^{-1} \mathbf{q} \quad (2)$$

Notice that  $V_A$  is the prescribed voltage on all spheres in the model while the external sphere is held at  $V_B$ . The effects of varying the voltage on different spheres in the model have not been analyzed, but since the modeled conducting spacecraft would be held at uniform voltage, this approach is a logical one, and also reduces the amount of modeled parameters.

The inverse of the position dependent capacitance matrix in Eq. (2),  $[C_M]^{-1}$ , can be expanded as follows, according to the nomenclature adopted in Figure 1, with  $\mathbf{r}_{i,B} = \mathbf{d} - \mathbf{r}_i$ :

$$[C_M]^{-1} = \begin{bmatrix} 1/R_1 & 1/r_{1,2} & \cdots & 1/r_{1,n} & 1/r_{1,B} \\ 1/r_{2,1} & 1/R_2 & \ddots & \vdots & \vdots \\ \vdots & \ddots & \ddots & \vdots & \vdots \\ 1/r_{n,1} & \cdots & \cdots & 1/R_n & 1/r_{n,B} \\ 1/r_{B,1} & \cdots & \cdots & 1/r_{B,n} & 1/R_B \end{bmatrix} \quad (3)$$

The next step is to solve for the array of charges  $\mathbf{q}$  from Eq. (2) by inverting this  $n + 1$  size symmetric matrix, a computation that becomes increasingly intensive when more spheres are used in the model. Coulomb's law can then be implemented to calculate the linear force between each charged sphere. Since the location of the spheres within the modeled body are held fixed with respect to each other, their equal and opposite contributions cancel. The total force  $\mathbf{F}$  and torque  $\mathbf{L}$  about the origin  $O$  on body  $A$  due to external sphere  $B$  that results is given by the following summations.

$$\mathbf{F}_O = k_c q_B \sum_{i=1}^n \frac{q_i}{r_{i,B}^3} \mathbf{r}_{i,B} \quad (4)$$

$$\mathbf{L}_O = k_c q_B \sum_{i=1}^n \frac{q_i}{r_{i,B}^3} \mathbf{r}_i \times \mathbf{r}_{i,B} \quad (5)$$

Note that while any origin can be chosen for body  $A$ , the force and torque in Eqs. (4) and (5) are now defined from this reference origin. While the developments above are sufficient for the parameter determination and verification in this paper, they will need to be expanded to determine the electrostatic kinetics between two bodies modeled using the Multi Sphere Method. This is done by replacing the external sphere  $B$  with a collection of spheres using the same formulation as for body  $A$ . The force and torque relations will then contain double summations. While the MSM does not provide an analytic solution for the Coulomb interactions for any number of spheres, due to the  $n + 1$  dimensional matrix inversion, this computation is much faster than current FEM solvers. As such, relative spacecraft motion due to inter-formation actuation can be predicted in real time and incorporated in control algorithms. We are left with the task of choosing optimal parameters of the sphere and verifying the fidelity of the model, which is the focus of the remainder of this paper.

## FEM Truth Data

Since complete analytic solutions are non-existent for the electrostatic interaction between generic conducting geometries, a reliable truth model is necessary to determine an optimal parameter set for the MSM and verify its accuracy. While the accuracy of the experimental verification of relative Coulomb motion is gaining ground,<sup>23</sup> the disturbance errors are still an order of magnitude larger than the small 3D shape effects for which this model hopes to compensate. A better option is to use a higher order numerical electrostatic solver for the truth data. Out of the wide range of commercially available electrostatic modeling software, Ansoft Maxwell 3D<sup>24</sup> is chosen for verification of the MSM due to its ability to resolve various field parameters (such as surface charge distribution, force and torque), parameter sweep capabilities, computationally efficient mesh refinement, and relative ease of use. Note that the MSM setup could be performed using any FEM electrostatic field solver to provide the three-dimensional force field input into the MSM optimization routine.

For this scenario a cylinder measuring 3 m in length by 1 m in diameter will be modeled because it represents a simple shape with significant 3D variation from a sphere, sized similar to popular GEO dual-spinner configurations. This cylinder and an external sphere with a 1 m diameter are created as solid three dimensional shapes in Maxwell, as shown in the left hand of Figure 2(a). Perfectly conducting material properties are assigned to both shapes, and a voltage excitation of +30 kV is prescribed on both. A large external surface held at zero voltage forms the remaining boundary condition. Next, the FEM software creates solutions for the electrostatic force and torque on the cylinder (or a more complex geometry), while the location of the external sphere is swept through the locations shown in Figure 2(b), which represent possible relative separation distances encountered in a spacecraft formation. Due to the symmetry of this particular shape, analysis is necessary in only one quadrant on any plane that intersects the cylinder's axis. This force and torque data set is exported to be used for a nonlinear fit that will search for the optimal sphere parameters. When the modeled shape and the external cylinder intersect, Maxwell returns an empty data point, which in turn is ignored by the nonlinear fit.

The force data retrieved from Maxwell cannot be compared directly to a lower order model at all relative positions. Remember that the Multi Sphere Model is based upon the position dependent capacitance charge model as outline in the previous section. This model does not capture the induced charge effects that result when the separation distance of two charged objects is very small. If this is the case, the repulsion or attraction causes the charge in each conductor to be shifted away from or towards the other object. As a result, the center of charge is not at the center of the object, which can change the magnitude of the forces and torques significantly. If the MSM is populated throughout its volume with many spheres, these induced charge effects may be captured. For the scope of this paper, however, the cylinder is populated with no more than three spheres, so the induced charge effects will not be captured in the radial dimension of the cylinder. Therefore, it is necessary to ignore the data points from Maxwell with separation distances that are small enough to contain induced charge effects. Secondly, when large separation distances are considered, the solution from Maxwell can be shown to contain numerical errors. To ensure that these anomalies do not affect the MSM solution, data points with large separation distances must also be removed.

In order to determine the upper and lower bounds of the separation distances that can be used for MSM verification, a simulation is run in Maxwell with two identical spheres, over the range of separation distances deemed reasonable above. This is compared to force values from the position dependent capacitance model laid out in Eqs. (1)-(5), as shown in Figure 3. Both spheres have a diameter of 1 m; one sphere is held at  $V_1 = +30$  kV while the other is allowed to vary through

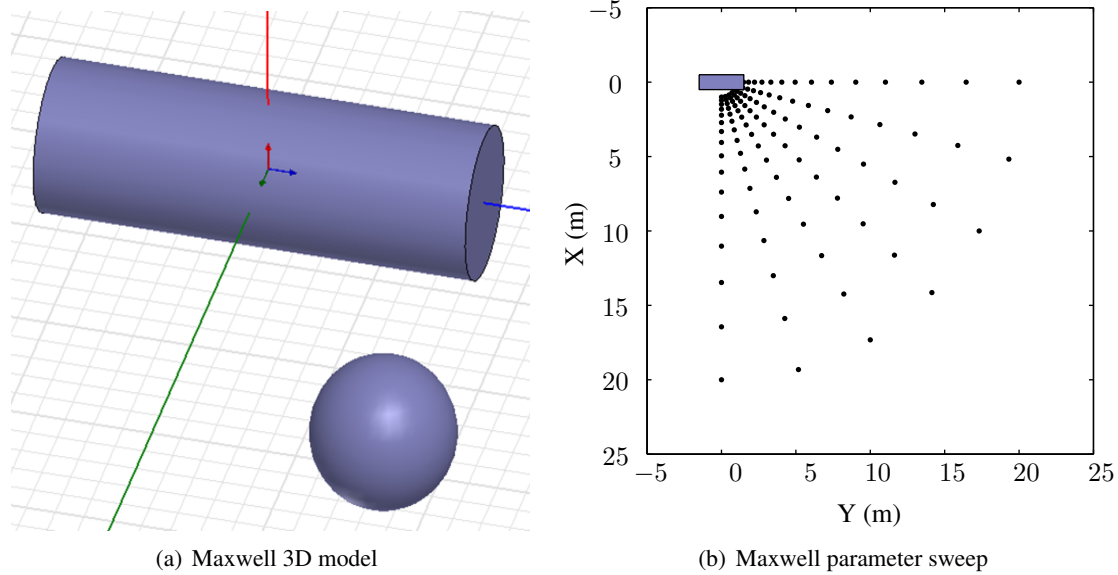


**Figure 2. Maxwell 3D model and parameter sweep for data export**

the voltages shown in the figure. In order to highlight the computational errors at large separation distances, the forces are plotted on a logarithmic scale. In this regime, the capacitive force model is assumed to be more accurate than the Maxwell data. At the small separation regime, the Maxwell data is known to be more accurate because induced effects are captured, but these data points shall be ignored when fitting parameters to the MSM because it is not expected to capture those effects. Notice that the discrepancy in induced effects is least when both spheres have equal charge  $V = +30$  kV. For the parameter selection algorithm, the data points with separation distance from 2.2255 m to 13.4637 m will be used. When verifying the model with scaled voltage values, Figure 3 will be referenced to choose an appropriate range of separation distances.

### PARAMETER SELECTION ALGORITHM

For the MSM to be used effectively in a six degree of freedom simulation, a set of sphere parameters needs to be selected that best predicts the forces and torques on a given conductor shape over a full range of separation distances and orientations. An initial guess of the position and size of the spheres is chosen to model the geometry; this guess fixes the total number of spheres to be used. A nonlinear fitting scheme then compares the resulting forces and torques from the MSM to those of a trusted higher order solution (such as the FEM solver discussed above) and iterates on the parameter values until they converge to a model that optimally matches the trusted values.

### Symmetry Arguments

If  $n$  spheres are chosen to model a given spacecraft shape, the parameter selection algorithm needs to determine  $4n$  parameters (3 spatial coordinates and a radius for each sphere). If *a priori* knowledge of the modeled shape symmetry is considered, the number of unknown parameters can be reduced, which will significantly enhance the computational time of the parameter fit. Efficiency of the nonlinear fit is not crucial as it needs to be executed only once for a given spacecraft shape

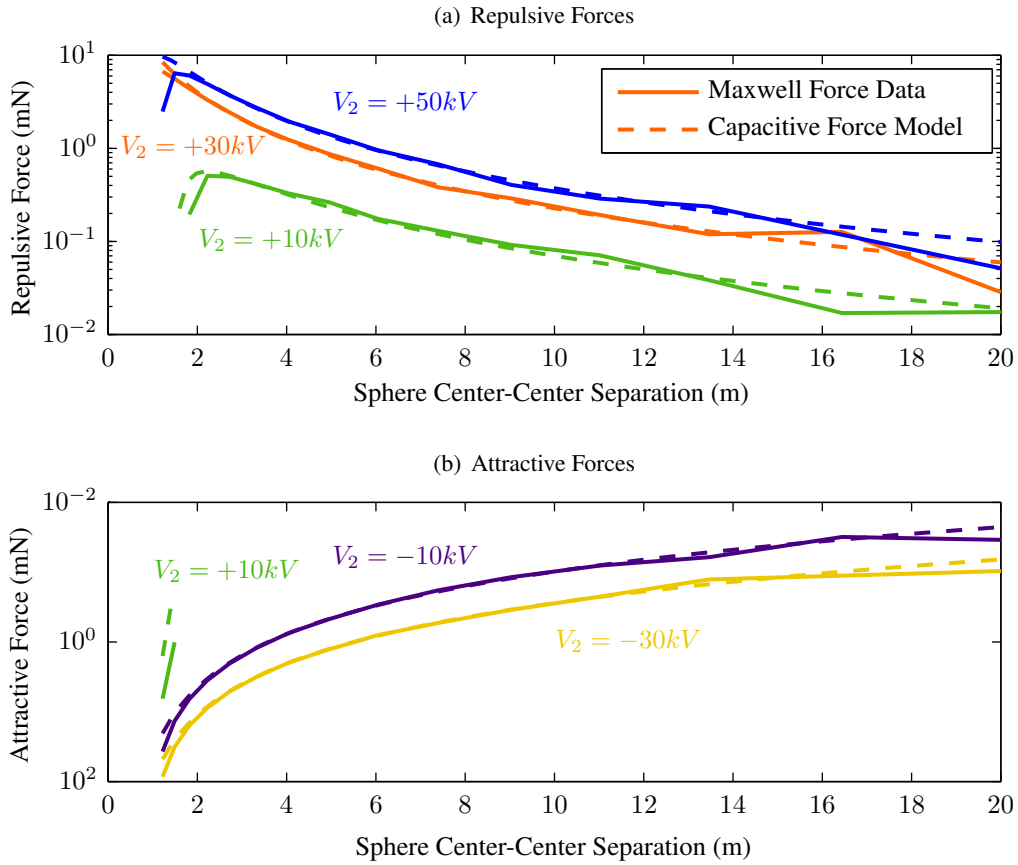


**Figure 3. Comparison between Maxwell force data and position dependent capacitance model forces**

preceding the model's use in simulations, but has aided considerably in the process of tuning the nonlinear fit.

For our purposes, all symmetry scenarios can be categorized as **axial** or **planar** symmetry. If the modeled spacecraft shape exhibits symmetry about a given axis, then any spheres that lie on this axis in the initial guess will remain there, thus eliminating the need to solve for off-axis coordinates. Any other spheres will be symmetrically rotated a predetermined  $p$  number of times around the axis. Planar symmetry is dealt with in a similar way - spheres lying on the plane will remain there, while off-planar spheres are mirrored across the plane. For the scenario in Figure 4, with axial and planar symmetries evident in the cylinder and  $p$  chosen to be 3, only two spheres need to be specified in the initial parameter guess, but seven spheres result in the final model. Moreover, the parameter space is reduced from 28 to just 4.

### Nonlinear Fit

If there is a linear relationship between the parameters of a system and the output of that system, a linear regression can be performed to find an optimal solution for those parameters that minimizes some error norm between the model output and a truth output. This is even possible if the system can be linearized, but in the case of the MSM, the capacitance matrix inversion prohibits a linearization of the system. The input in this case is the external sphere position, the outputs are the force and

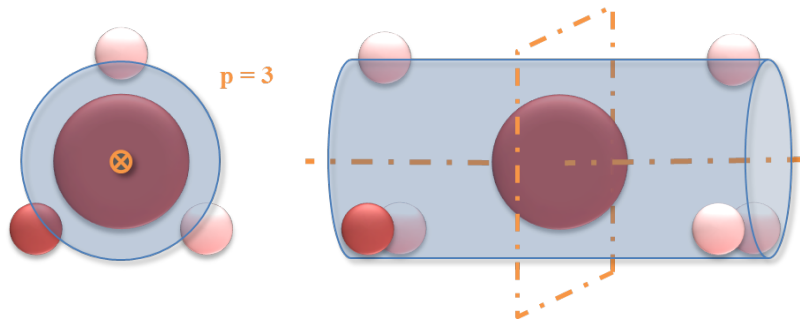


**Figure 4. Axial and planar symmetry considerations.**

torque values on the modeled body for that external sphere position, and the parameters are the sphere positions and sizes, as simplified by the symmetry arguments discussed above. A Gaussian least squares differential correction method is used to determine the optimal parameter set for the MSM.<sup>25</sup> Normally, this method requires partial derivatives of the model output function with respect to the parameters. The matrix inversion in the MSM model also prevents an analytical form of these partials, so a finite difference method is used.

This entire Gaussian least squares differential correction algorithm is performed by the nonlinear fit function ‘nlinfit’ in MATLAB. This function iteratively refits a weighted nonlinear regression, where the weights at each iteration are based on each observation’s residual from the previous iteration. These weights serve to down-weight points that are outliers so that their influence on the fit is decreased. Iterations continue until the weights converge.<sup>26,27</sup> There are various weighting algorithms to determine the optimal solution, of which the standard bi-square function is used. Moreover, the relative weight of each data point can be prescribed which is useful if fitting to the correct forces is more important than obtaining accurate torques, for example. As with any nonlinear fit, global convergence of the optimal solution is dependent on the initial guess of the sphere parameters. A manual search is used to determine an appropriate set of initial parameters. Although the symmetry arguments as implemented above aid in the computation effort, this approach can break down when the model consists of many spheres. Other schemes to populate a given geometry with numerous spheres are being investigated. However, as shown with the results below, this MSM approach is yielding practical and implementable solutions.

## MODEL VERIFICATION

The algorithms described above are run to determine the optimal MSM parameters to model the electrostatic interactions of the aforementioned 1 m diameter by 3 m length cylinder. An initial guess with three spheres is chosen, where the center sphere lies at the origin and the mirrored side spheres lie along the  $y$ -axis. Remember that not the entire range of locations shown in Figure 2(b) is used in the fit, but only the separation distances deemed accurate by Figure 3. That is, those with a surface to surface separation greater than 1 m and with a center to center separation smaller than or equal to 13.4637 m.

The geometry of the resulting spheres, superimposed on the actual cylinder, is shown in Figure 5, with parameters listed in Table 4. This model will be used throughout the remainder of the paper.

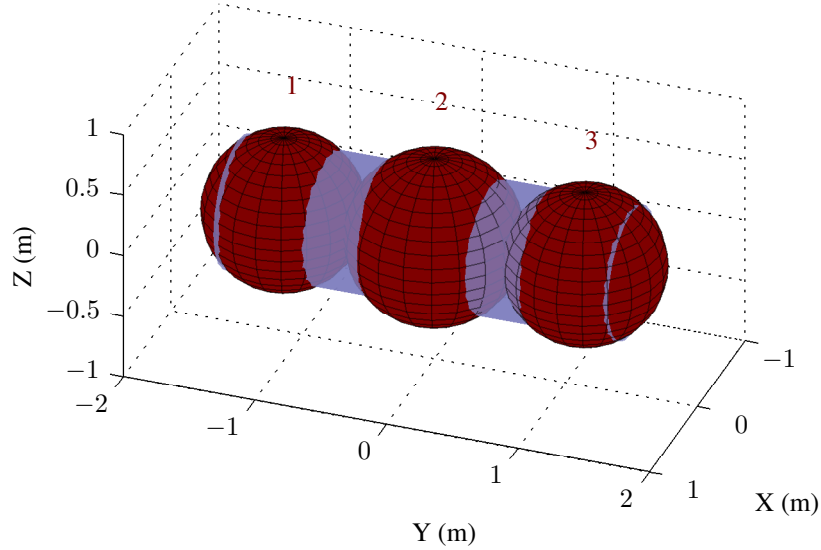


**Figure 5. Multi Sphere Model parameters for cylinder geometry**

**Table 1. Parameters of three sphere MSM for cylinder**

	Sphere 1	Sphere 2	Sphere 3
X Coordinate (m)	0	0	0
Y Coordinate (m)	-1.1454	0	1.1454
Z Coordinate (m)	0	0	0
Radius (m)	0.5959	0.6534	0.5959

### Quantifying Fit

A large effort in the current research is in verifying the quality of the aforementioned linear fit. Once a set of parameters is chosen, the accuracy of the model compared to numerical results from Maxwell must be determined. While the nonlinear fit returns a mean squared error norm that can be used to compare the quality of one fit to another, it is desirable to analyze in more details where in the physical space surrounding the geometry a particular MSM parameter solution fits the Maxwell data well or poorly.

Figures 6 and 7 show the visual metric that is used to analyze the quality of a given parameter set, for forces and torques respectively. In Figure 6(a), the output values from the MSM are plotted against the numerical truth model (Maxwell) at each external sphere position, with a line of slope 1 to show the desired position of data points. Data points within the region used for parameter selection are shown in black, while extraneous points are shown in red. While this plot shows that the current MSM over-predicts the higher forces, it does not contain any information about where these over-predictions occur, although we can gather that this happens when the external sphere is closer to the cylindrical body. Figure 6(b) displays the interpolated absolute error at a given external sphere position on the  $x$ - and  $y$ -axis, using a logarithmic color scale. Because the model does not capture induced effects, which causes a decrease in the repulsion between very close like-charged objects, it over-predicts the magnitude of forces at very close separation distances. Similarly, the

torques at locations shown in red are not very accurately captured by the model. This justifies the use of only the accurate data points in the middle of the range from Maxwell for the MSM parameter fit.

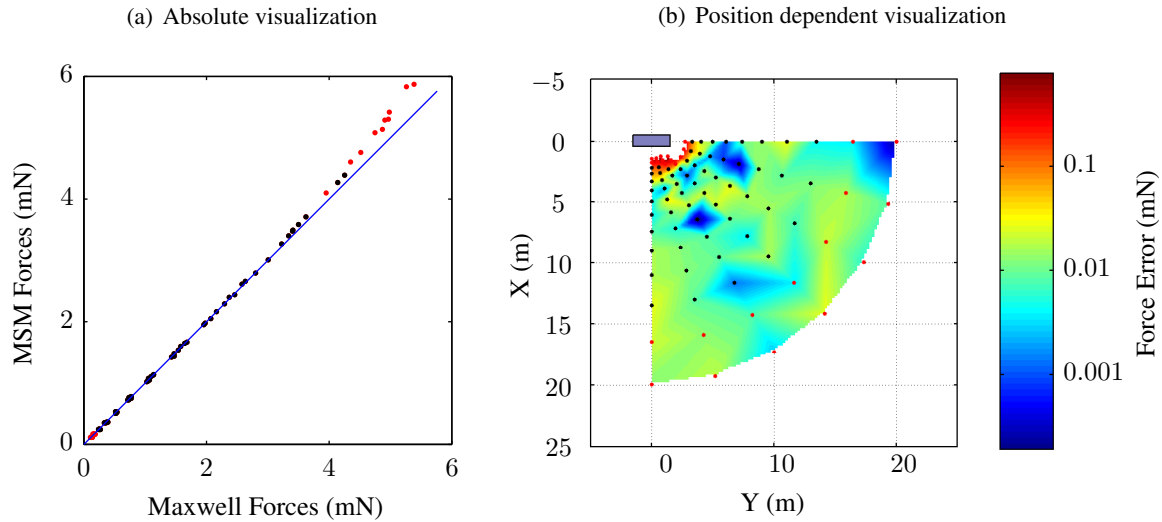


**Figure 6. Force comparison - MSM and Maxwell**

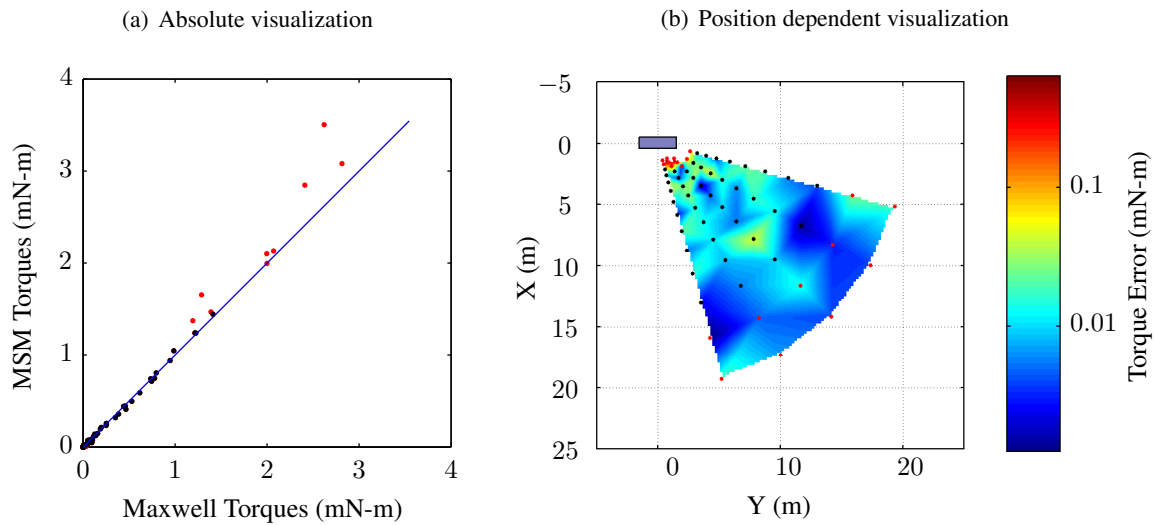


**Figure 7. Torque comparison - MSM and Maxwell**

While the visual approach to quantifying the MSM model above is useful for analyzing the quality of a single parameter fit, when multiple scenarios are compared to each other, it is desirable to have a single value for the quality of the fit for each scenario. The following scalar residual sum is therefore defined, where  $n$  is the number of external sphere locations  $d_i$  deemed not to capture induced effects or numerical anomalies as in Figure 3:

$$RES_F = \frac{\sum_{i=1}^n |F_{MSM}(\mathbf{d}_i) - F_{truth}(\mathbf{d}_i)|}{\sum_{i=1}^n F_{truth}(\mathbf{d}_i)} \quad (6)$$

$$RES_L = \frac{\sum_{i=1}^n |L_{MSM}(\mathbf{d}_i) - L_{truth}(\mathbf{d}_i)|}{\sum_{i=1}^n L_{truth}(\mathbf{d}_i)} \quad (7)$$

Dividing by the denominator ensures that this scalar residual sum is independent of the resolution of the data set. Table 2 compares the residuals of the three sphere MSM fit shown above and a single sphere model (referred to as the effective sphere method in Reference 22). The single sphere size is determined using the same non-linear fit, resulting in  $R = 0.9974$  m. It is clear that the single sphere results in much higher residuals than the three sphere model, and  $RES_L$  for a single sphere is unity because it lacks the ability to predict any non-zero torques.

**Table 2. Scalar residual comparison between three sphere MSM and single sphere model**

	3 sphere MSM	Single sphere model
$RES_F$	0.0155	0.0972
$RES_L$	0.0485	1.0000

### Model Scaling

An important step to validating the Multi Sphere Model is to verify whether it scales with some of the arbitrary constants that were chosen when using Maxwell to develop a truth model data set. While the geometry of the modeled shape is specified in the problem statement, the size of the external sphere  $R_B$  and the model and external sphere voltage  $V_A$  and  $V_B$ , were chosen fairly arbitrarily, though they represent typical spacecraft charging parameters. When the MSM is utilized in simulations, these conditions are liable to change. Moreover, the external sphere could take on a generic 3D shape of its own, which can in turn be modeled with the MSM. To verify that the model holds when these parameters are changed, the outputs of the MSM with the optimized sphere parameters are compared to numerical simulations while individually varying the parameters  $R_B$ ,  $V_A$  and  $V_B$  and replacing the external sphere with a duplicate of the 3D body at two orientations. Remember that the nominal values are an external sphere with  $R_B = 0.5$  m,  $V_A = V_B = 30$  kV. The results are concisely summarized using scalar residual values in Table 3.

The residual values for all the scaled scenarios are an improvement over the single sphere residuals in Table 2. The only scenario that yields less than desirable results are the combination of  $V = +30$  kV and  $V = +10$  kV. Figure 3 shows that the induced charge effects are largest for this combination of charges, which are not captured by a three sphere MSM. Future models with multiple spheres may capture these effects better. For now, it is still clear that the three sphere model provides an improvement over other models because of its ability to resolve torques and forces more accurately than a single sphere approximation.

**Table 3. Scalar residual comparison of scaled parameter variation from numerical simulation**

$R_B$ variation	0.25 m	1m	
$RES_F$	0.0150	0.0578	
$RES_L$	0.0639	0.0749	
$V_A$ variation	-30 kV	10 kV	50 kV
$RES_F$	0.0281	0.0225	0.0242
$RES_L$	0.0370	0.1021	0.0745
$V_B$ variation	-30 kV	10 kV	50 kV
$RES_F$	0.0275	0.0733	0.0241
$RES_L$	0.0424	0.2454	0.0481
External cylinder	Parallel	Perpendicular	
$RES_F$	0.0355	0.0305	
$RES_L$	0.0350	0.0744	

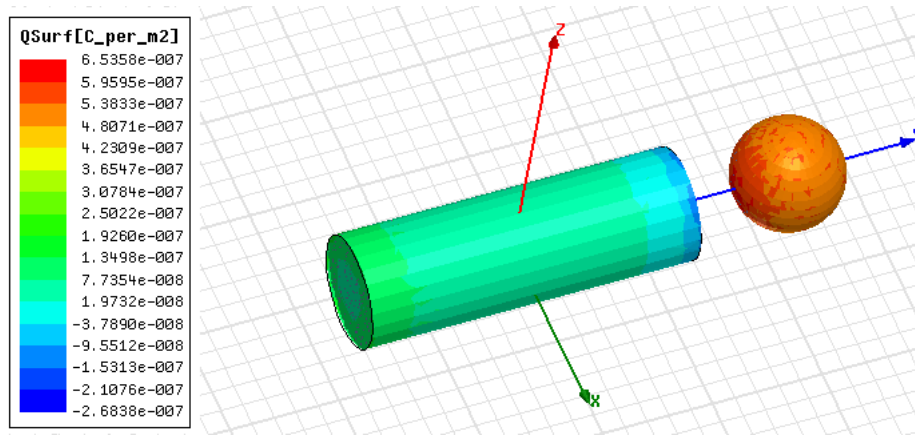
### CHARGE DISTRIBUTION IN MSM

The claim was made earlier that the Multi Sphere Model captures induced charge effects that are not included in the analytic 2-sphere solution with position dependent capacitance considerations, but only in a dimension with multiple spheres. To verify this claim, a comparison is shown in Figure 8 between the charge distribution on the objects in Maxwell for an external sphere in line with the cylinder, compared with the three sphere MSM in the same orientation. To maximize the induced effects, the cylinder is given a voltage  $V_A = 10$  kV while the external sphere has  $V_B = 30$  kV prescribed. Clearly, the distribution of charge in the three spheres that compose the MSM matches the charge distribution in the fully resolved geometry shown in Maxwell. Where a single sphere model would place all the charge at the center of the body, the MSM has extra freedom in where the charges are distributed along the y-axis, thus capturing some of the induced charge effects.

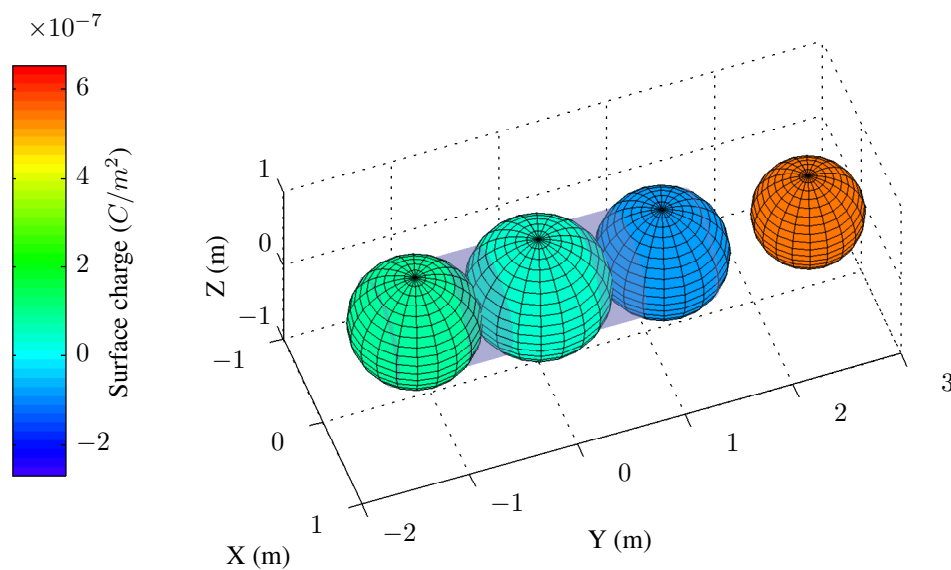
### CYLINDER DE-SPIN SIMULATION

In order to demonstrate the practicality of the Multi Sphere Model, a simulation is performed whereby a sphere is used to remove the angular rotation on a cylinder using only charge control. Since this scenario requires real-time knowledge of electrostatic torques, the MSM is the only non-FEM model that can achieve this simulation, and performs it many orders of magnitude faster. A uniform density  $3 \text{ m} \times 1 \text{ m}$  cylinder (as before) is placed in deep space at a constant separation distance  $d = 10$  m from a sphere of radius  $R = 0.5$  m, with orientation defined as in Figure 9. The cylinder is held at a constant voltage  $V_1 = -30$  kV, while the sphere's voltage is allowed to vary between  $0 \text{ kV} < V_2 < 30 \text{ kV}$ . This scenario represents a spacecraft (the sphere) that flies in proximity of a debris object (the cylinder). These voltages can be implemented by using an electron gun to keep the debris cylinder at constant negative charge, while using another charge control device to control the spacecraft's own voltage.<sup>2</sup> The simulation assumes that a separate relative motion feedback control maintains a stationary relative location. This allows the study to focus on impact of the electrostatic torques.

The cylinder is allowed to rotate about its center, in the plane that it makes with the sphere, and given an initial angular velocity  $\omega_0 = 2$  deg/s. The voltage on the neighboring sphere is varied



(a) Surface charge from Maxwell 3D



(b) Surface charge from three sphere MSM

**Figure 8. Surface charge density comparison between Maxwell 3D and a three sphere MSM**

according to the sign-modified PD control law in Eq. (8) in order to bring the cylinder to rest perpendicular to the sphere (at  $\theta = 90$  deg).

$$V_2 = V_{2,\max}\{P|\sin(\theta)| + D\text{sign}(\theta)\omega\} \quad (8)$$

This voltage control is chosen such that it always creates a torque which opposes the space debris spin. The sphere is limited to voltage polarities opposite that of the cylinder because if indirect charging is employed, having a  $\pm 30$  kV potential on each object would require at least a 60 kV electron gun potential. The chosen control allows the craft potentials to be saturated at  $V_{2,\max}$ . Simulation parameters are given in Table 4, while Figure 10 shows the de-spin results.

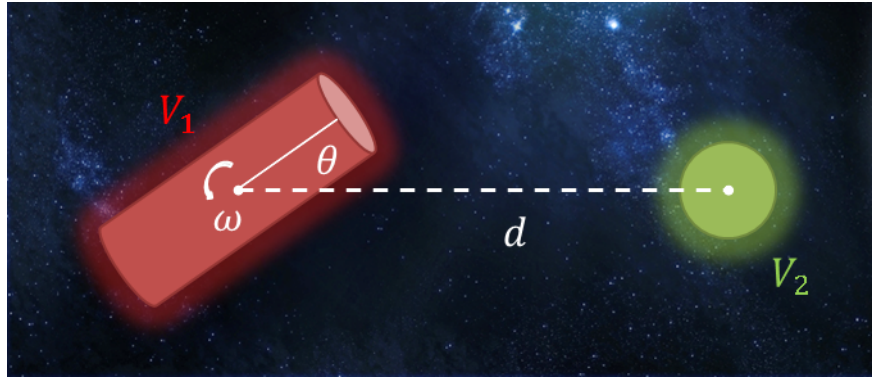


Figure 9. Depiction of cylinder de-spin simulation

Table 4. Parameters for cylinder de-spin simulation

Parameter	Value	Units	Description
$d$	10	m	Object center-to-center separation
$\rho$	100	kg/m <sup>2</sup>	Object densities
$m_1$	235.6	kg	Cylinder mass
$I_{1,x}$	191.4	kg·m <sup>2</sup>	Cylinder transverse moment of inertia
$I_{1,y}$	29.5	kg·m <sup>2</sup>	Cylinder axial moment of inertia
$V_1$	-30	kV	Cylinder constant voltage
$V_{2,max}$	+30	kV	Sphere maximum voltage
$P$	1		Control law proportional gain
$D$	500		Control law derivative gain
$\omega_0$	2	deg/s	Initial cylinder angular velocity

A three sphere MSM with the parameters determined earlier is used to determine the Coulomb interactions during the simulation. It takes roughly 70 hours for the cylinder to stop making complete rotations. A 2 deg/s initial rotation is not especially large, but considering the relatively large prescribed separation distance and the time scale of most space maneuvers, this is a very promising result for the de-spin of a debris object.

From Figure 7, the three sphere MSM is shown to approximate the torques to within 30% of the truth value from Maxwell for a 10 m separation distance. This discrepancy is to be expected since the nominal torques at this separation distance are very small, and computational errors are present in Maxwell. To analyze the effects of torque uncertainties, the simulation was re-run using a 30% increase and decrease in the torque value used to resolve the dynamics. When the MSM in the controller under-predicted the torque value, it takes 18% less time for the debris object to stop making full rotations, but removing the remaining oscillations is slower. If the MSM over-predicts the actual torque values, the debris takes 31% longer to despin, but the asymptotic convergence to zero motion occurs in roughly the same amount of time. These are the extremes for model uncertainty.

## CONCLUSION

This paper introduces the Multi Sphere Model (MSM), a reduced order, computationally efficient electrostatic model that captures the three dimensional Coulomb effects of generic conducting

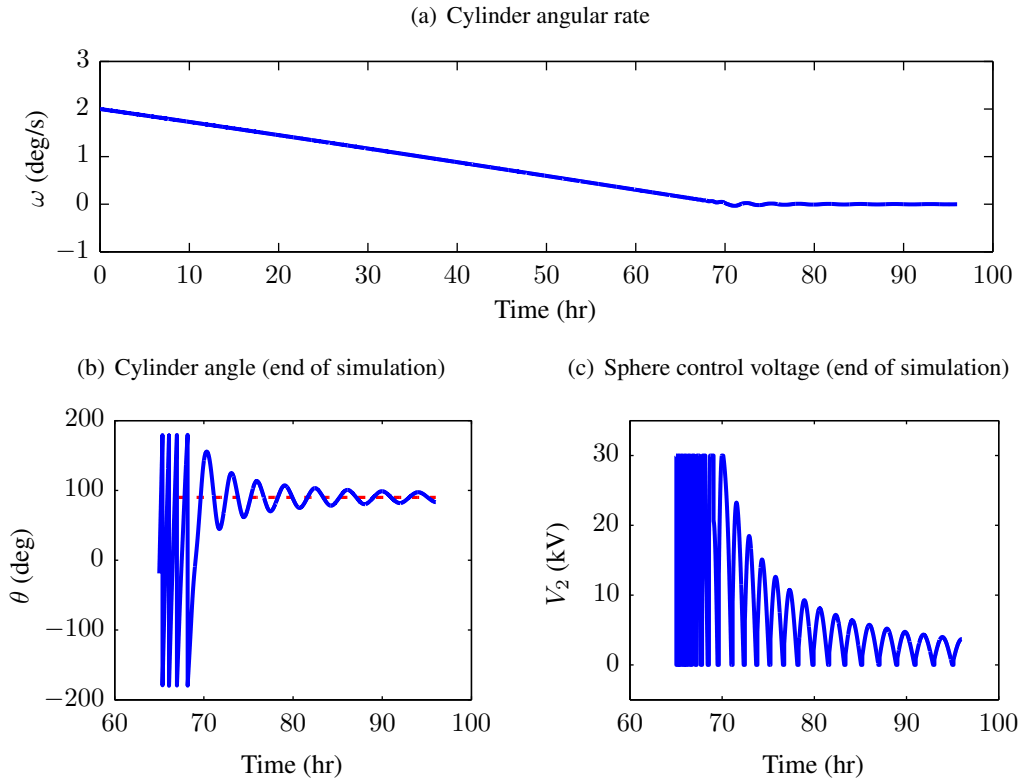


**Figure 10. Cylinder de-spin simulation using voltage control on proximity sphere**

shapes. A commercially available finite element analysis software suite is used as a truth model to determine the optimal size and position of the spheres that comprise the model. Symmetry arguments are included to decrease the computational intensity of the nonlinear fit. The MSM is an improvement over previous finite sphere models because it embodies higher order orientation dependent electrostatic effects and can resolve electrostatic torques on a three dimensional body. The accuracy of the model is numerically studied, and the MSM is demonstrated to be robust for a given geometry when other parameters are varied. Moreover, it is shown that a model with many spheres will capture higher order induced charge effects that are not inherent in a position dependent capacity model for two spheres. Using the MSM, 6-DOF Coulomb formation flying scenarios can be simulated, which will eventually aid in developing control strategies. A simple example is given where a voltage-controlled sphere is used to de-spin a nearby 3D object. Future work involves new ways to populate a given shape with spheres to ensure global optimal parameters, as well as expanding the model to include plasma effects and dielectric spacecraft materials.

## REFERENCES

- [1] J. H. Cover, W. Knauer, and H. A. Maurer, "Lightweight Reflecting Structures Utilizing Electrostatic Inflation," US Patent 3,546,706, October 1966.
- [2] L. B. King, G. G. Parker, S. Deshmukh, and J.-H. Chong, "Spacecraft Formation-Flying using Inter-Vehicle Coulomb Forces," tech. rep., NASA/NIAC, January 2002. <http://www.niac.usra.edu>.
- [3] L. B. King, G. G. Parker, S. Deshmukh, and J.-H. Chong, "Study of Interspacecraft Coulomb Forces and Implications for Formation Flying," *AIAA Journal of Propulsion and Power*, Vol. 19, May–June 2003, pp. 497–505.

- [4] H. Schaub, G. G. Parker, and L. B. King, "Challenges and Prospect of Coulomb Formations," *Journal of the Astronautical Sciences*, Vol. 52, Jan.–June 2004, pp. 169–193.
- [5] H. Schaub and D. F. Moorer, "Geosynchronous Large Debris Reorbiter: Challenges and Prospects," *AAS Kyle T. Alfriend Astrodynamics Symposium*, Monterey, CA, May 17–19 2010. Paper No. AAS 10-311.
- [6] H. Schaub and L. E. Z. Jasper, "Circular Orbit Radius Control Using Electrostatic Actuation for 2-Craft Configurations," *AAS/AIAA Astrodynamics Specialist Conference*, Girdwood, Alaska, July 31 – August 4 2011. Paper AAS 11–498.
- [7] E. Hogan and H. Schaub, "Relative Motion Control for Two-Spacecraft Electrostatic Orbit Corrections," *AAS/AIAA Spaceflight Mechanics Meeting*, Girdwood, Alaska, July 31 – August 4 2011. Paper AAS 11–466.
- [8] A. C. Tribble, *The Space Environment - Implications for Spacecraft Design*. Princeton University Press, revised and expanded ed., 2003.
- [9] M. H. Denton, M. F. Thomsen, H. Korth, S. Lynch, J. C. Zhang, and M. W. Liemohn, "Bulk plasma properties at geosynchronous orbit," *Journal of Geophysical Research*, Vol. 110, 07 2005.
- [10] J. Berryman and H. Schaub, "Analytical Charge Analysis for 2- and 3-Craft Coulomb Formations," *AIAA Journal of Guidance, Control, and Dynamics*, Vol. 30, Nov.–Dec. 2007, pp. 1701–1710.
- [11] H. Vasavada and H. Schaub, "Analytic Solutions for Equal Mass Four-Craft Static Coulomb Formation," *Journal of the Astronautical Sciences*, Vol. 56, Jan. – March 2008, pp. 17–40.
- [12] E. Hogan and H. Schaub, "Collinear Invariant Shapes for Three-Craft Coulomb Formations," *AAS/AIAA Astrodynamics Specialist Conference*, Toronto, Canada, Aug. 2–5 2010. AIAA-2010-7954.
- [13] G. G. Parker, C. E. Passerello, and H. Schaub, "Static Formation Control using Interspacecraft Coulomb Forces," *2nd International Symposium on Formation Flying Missions and Technologies*, Washington D.C., Sept. 14–16, 2004 2004.
- [14] H. Schaub, C. Hall, and J. Berryman, "Necessary Conditions for Circularly-Restricted Static Coulomb Formations," *Journal of the Astronautical Sciences*, Vol. 54, July-Dec. 2006, pp. 525–541.
- [15] H. Schaub, "Stabilization of Satellite Motion Relative to a Coulomb Spacecraft Formation," *Journal of Guidance, Control and Dynamics*, Vol. 28, Nov.–Dec. 2005, pp. 1231–1239.
- [16] A. Natarajan and H. Schaub, "Linear Dynamics and Stability Analysis of a Coulomb Tether Formation," *Journal of Guidance, Control, and Dynamics*, Vol. 29, July–Aug. 2006, pp. 831–839.
- [17] C. R. Seubert and H. Schaub, "One-Dimensional Testbed for Coulomb Controlled Spacecraft Studies," *AAS/AIAA Spaceflight Mechanics Meeting*, Savannah, Georgia, Feb. 8–12 2009.
- [18] C. R. Seubert and H. Schaub, "Closed-Loop One-Dimensional Charged Relative Motion Experiments Simulating Constrained Orbital Motion," *AAS/AIAA Astrodynamics Specialist Conference*, Pittsburgh, PA, Aug. 9–13 2009.
- [19] W. R. Smythe, *Static and Dynamic Electricity*. McGraw–Hill, 3rd ed., 1968.
- [20] J. Sliško and R. A. Brito-Orta, "On approximate formulas for the electrostatic force between two conducting spheres," *American Journal of Physics*, Vol. 66, No. 4, 1998, pp. 352–355.
- [21] J. A. Soules, "Precise Calculation of the Electrostatic Force Between Charged Spheres Including Induction Effects," *American Journal of Physics*, Vol. 58, No. 12, 1990, pp. 1195–1199.
- [22] L. E. Z. Jasper and H. Schaub, "Effective Sphere Modeling for Electrostatic Forces on a Three-Dimensional Spacecraft Shape," *AAS/AIAA Spaceflight Mechanics Meeting*, Girdwood, Alaska, July 31 – August 4 2011. Paper AAS 11–465.
- [23] C. R. Seubert and H. Schaub, "Electrostatic Force Model for Terrestrial Experiments on the Coulomb Testbed," *61st International Astronautical Congress*, Prague, CZ, International Astronautical Federation, Sept. 2010. Paper IAC-10.C1.1.9.
- [24] ANSYS, *Maxwell 3D Software*. 2010. Version 13.0.0. <http://www.ansoft.com/products/em/maxwell>.
- [25] J. Junkins, *Optimal Estimation of Dynamical Systems*. Sijthoff-Noordhoff, 1st ed., 1978.
- [26] W. H. DuMouchel and F. L. O'Brien, "Integrating a Robust Option into a Multiple Regression Computing Environment," *Computer Science and Statistics: Proceedings of the 21st Symposium on the Interface*, Alexandria, VA, American Statistical Association, 1989.
- [27] P. Holland and R. Welsch, "Robust Regression Using Iteratively Reweighted Least-Squares," *Communications in Statistics: Theory and Methods*, No. A6, 1977, pp. 813–827.